

TURBULENT SCALAR TRANSFER AND ITS DEPENDENCE ON THE SCHMIDT NUMBER

P. Orlandi

Dipartimento di Meccanica e Aeronautica
Via Eudossiana 16, Roma Italy
orlandi@kolmogorov.ing.uniroma1.it

R. A. Antonia

Discipline of Mechanical Engineering
University of Newcastle
N.S.W., 2308 Australia
robert.antonio@newcastle.edu.au

ABSTRACT

Direct numerical simulations (DNSs) of decaying isotropic turbulence with a passive scalar at different Schmidt numbers show that the Kolmogorov and Batchelor scaling collapse the high wavenumber region of the spectra and transfer functions effectively. There is a k^{-1} range for the inertial-diffusive range at small R_λ for $Sc \geq 1$. To gain some information at a higher R_λ , EDQNM simulations are used, after validation at small R_λ against the DNS. Although the different inertial ranges yield slopes that differ slightly from those predicted by theoretical arguments, the scaling and variation in slope between inertial and inertial-diffusive ranges are adequately reproduced by the EDQNM. The pdf of some of the terms in the transport equation for θ^2 provides some insight into which term is responsible for the formation of large radius of curvature scalar gradient regions.

INTRODUCTION

Mixing of a passive scalar is implemented much more efficiently by turbulent than laminar flows. Understanding the complexity of turbulent mixing has important implications for many engineering applications. For example, since the dynamics of the scalar small scales play an important role in combustion, their adequate understanding is an important prerequisite to controlling turbulent combustion. At present, full direct simulations are out of reach of current computers. The only approach is to rely on LES, where small scales are modeled. Realistic scaling of the small scales which accounts for the effects of the turbulent Reynolds number R_λ and the Schmidt number Sc ($\equiv \nu/\nu_\theta$, where ν is the kinematic viscosity and ν_θ is the diffusivity of the scalar) should help in fine tuning sub-grid-scale closures. To better understand the behavior of the passive scalar dynamics at high Reynolds numbers, analytical turbulence theories, such as the EDQNM (Eddy Damped Quasinormal Markovian) approach, can be of help. This approach is described in Lesieur (1987) and has been recently applied by Herr *et al.* (1996) to passive scalars with a mean gradient.

In the present study, direct numerical simulations (DNS) of decaying isotropic turbulence with a passive scalar have been carried out over a range of small R_λ (maximum of about 70) for Sc equal to 1 and 3. Previous results (Antonia & Orlandi (2003a,b)) at a smaller R_λ , but with a wider

range of Sc (0.07 to 15) have also been used. The data base is used to gain some insight into the transfer of the scalar from large to small scales. This transfer, together with that of the kinetic energy, is at the root of the complex nature of turbulence. The Navier-Stokes equations, when expressed in the spectral domain, suggest that the transfer is made up of all the triadic interactions. These can be readily computed via DNS.

For the EDQNM theory, closure of the triadic interactions is necessary. The interesting feature of this theory is that the smallest and largest scales can be widely separated. The increment in the wavenumber interval can be increased in octave steps, with a concomitant reduction in computational time. The evolution equations for the spectra are solved with a closure that models the complex interaction between the structures (phases). In the past, for high Reynolds numbers, spectral closures have been validated by comparison with LES results (Herring (1990)). Here the validation of the EDQNM is against DNS at a small Reynolds number. One objective is to ascertain the most appropriate scaling for the energy and scalar spectra and their relative transfer functions. The spectral closures can be used at relatively high Sc and R_λ and therefore permit a more suitable comparison with the predictions of Kolmogorov and Batchelor. For decaying turbulence, DNS cannot yield a $k^{-5/3}$ inertial range due to current computer limitations. DNS can however, at small R_λ and moderately high Sc , allow the k^{-1} range of Batchelor to be tested. It should be recalled that, according to Batchelor, the k^{-1} range should exist even in the absence of an inertial range.

EDQNM has been used to study relatively high Reynolds number flows. Similarly to Herring (1990), we have observed that the spectral closure does not reproduce a $k^{-5/3}$ range at moderate R_λ . The experiments of Mydlarski & Warhaft (1996) have indicated that $k^{-5/3}$ is approached only when R_λ is about 10^4 . To our knowledge, there has been not yet been an attempt to check if EDQNM can reproduce these experimental observations. Because of lack of space we will not address this issue here; it will be the subject of a future paper. The highest R_λ here consider in the present paper is only about 200 and, accordingly, we do not have a $k^{-(5/3)}$ range; instead, we observe a $k^{-1.5}$ range, which is consistent with the compensated spectra reported by Herring (1990).

PHYSICAL MODEL

The DNS is based on the Navier-Stokes equations and transport equations for a passive scalar. These equations are well known and not reproduced here; instead, a few comments are made with respect to the numerical method. Almost all DNSs of isotropic turbulence were implemented using pseudospectral methods; here, a second-order finite difference scheme is used (Orlandi (2000)). It is generally felt that second-order accuracy is too dissipative, leading to a faster decay of the spectra in the dissipation range. We would like to dispel this view by comparing our energy spectra with those reported by Wray (1999). Since there is an influence of initial conditions on the time history, the comparison can be done only with scaled spectra. To further assess the quality of our numerical method, the comparison is also extended to the energy transfer function. Orlandi & Antonia (2002) showed that scalar spectra at $Sc = 7$, as obtained by the two methods, follow each other closely. The transfer of energy $T(k)$ has been calculated using

$$T(k) = 2\nu k^2 E(k) + \frac{\partial E(k)}{\partial t} \quad (1)$$

This is an indirect calculation; the direct way consists in evaluating the triadic interactions from wavenumber space variables. Using a pseudospectral code, we verified that direct and indirect calculations of $T(k)$ agreed well with each other.

In the EDQNM, Eq.(1) can be solved if an expression for $T(k)$ as a function of $E(k)$ can be derived from the Navier-Stokes equations. Such an expression is given by Lesieur (1987). The integral of $T(k)$ must satisfy conservation properties. Using a special transformation, Crocco & Orlandi (1985) showed that these properties can be verified readily. The transformation maps the $p-q$ semi-infinite domain into a $\beta-\gamma$ triangular domain. In the $T(k)$ expression, there is a 'damping function' where a constant C_λ appears. Different expressions have been proposed. Here, we adopt the expression of Orszag (1970), i.e. $\eta(k) = \nu k^2 + C_\lambda [k^3 E(k)]^{1/2}$, which includes a local effect, instead of $\eta(k) = \nu k^2 + C_\lambda \int k^2 E(k) dk$. The latter expression gives a stronger damping at high k with too fast a rate of decay of the spectrum. The expression for $T(k)$ is not reported here.

The evolution of $E_\theta(k)$ is obtained by

$$\frac{\partial E_\theta(k)}{\partial t} = T_\theta(k) - 2\frac{\nu}{Sc} k^2 E_\theta(k) \quad (2)$$

where the expression for $T_\theta(k)$ in the new variables β and γ can be obtained from equation (VII-12-14) on Pg.260 in Lesieur (1997). It is

$$T_\theta(k) = \frac{1}{k} \int_0^1 d\beta \int_{1-\beta}^{1+\beta} d\gamma [S_\theta^+(k, \beta, \gamma) - S_\theta^-(k, \beta, \gamma)] \quad (3)$$

with

$$S_\theta(k, \beta, \gamma) = k^4 B_\theta(\beta, \gamma) D_\theta(k, \beta, \gamma) \frac{E(\gamma k)}{\gamma^2} \left[\frac{E_\theta(\beta k)}{\beta^2} - E_\theta(k) \right] \quad (4)$$

where

$$S_\theta^+(k, \beta, \gamma) = S_\theta(k, \beta, \gamma), \quad S_\theta^-(k, \beta, \gamma) = S_\theta\left(\frac{k}{\beta}, \beta, \gamma\right) \quad (5)$$

The geometrical factor and the relaxation frequency are

$$B_\theta(\beta, \gamma) = \frac{\beta}{4\gamma} [1 - (\gamma - \beta)^2][(\gamma + \beta)^2 - 1] \quad (6)$$

$$D_\theta(k, \beta, \gamma) = \frac{1 - e^{-[\zeta(k) + \zeta(\beta k) + \zeta(\gamma k)]t}}{\zeta(k) + \zeta(\beta k) + \zeta(\gamma k)} \quad (7)$$

The expression for $\zeta(\tilde{k})$ is similar to that for $\eta(\tilde{k})$ but for $\tilde{k} = \beta k$ and $\tilde{k} = k$, instead of ν , appears ν/Sc .

Eqs.(1) and (2) advance in time by a semi-analytical scheme (Herring & Kraichnan (1972)) that allows a time step greater than that possible by the low storage third-order Runge-Kutta scheme used in DNS. As described in Crocco & Orlandi (1985), the time step can be increased with a predictor-corrector scheme. To obtain the solution at higher Re and Sc , starting from $E(k) = E_\theta(k) = \left(\frac{q^2}{2}\right) \frac{128}{3} \left(\frac{k^4}{k_P^4}\right) \exp(-4\frac{k}{k_P})$, in the first short period of time there is a build-up of energy and scalar dissipation rate at high k , due to the transfer from low to high k . In this short period, the total kinetic energy $q^2/2 = \int E(k) dk$ and scalar variance $\theta^2/2 = \int E_\theta(k) dk$ remain constant. However, the energy and scalar dissipation rates grow and, consequently, a very small time step is required. To speed up the simulation, a time transformation allows the time step to be increased when the power-law decay begins.

Scaling

In simulations of decaying turbulence, it is important to identify the most appropriate scaling variables and test the different types of similarity solutions that have been proposed. There is strong evidence in the literature in support of a Kolmogorov scaling for $E(k)$ and a Batchelor scaling for $E_\theta(k)$ when the wavenumber is large. On the other hand, George (1992a,b) proposed an equilibrium similarity theory with a scaling based on the Taylor velocity and scalar microscales λ and λ_θ and the turbulent energy and scalar variance. In this case, similarity applies to all scales of motion and, unlike the earlier asymptotic results of Karman & Howarth (1938) and others, is possible both for small values of R_λ and when R_λ decreases with time. This similarity is currently being assessed using the present DNS database.

The Kolmogorov scaling (indicated by the superscript $*$), based on ν and $\eta = (\frac{\nu^3}{\epsilon})^{1/4}$ ($\epsilon = 2\nu \int k^2 E(k) dk$) when applied to Eq.(1) gives

$$\frac{\partial E^*}{\partial t^*} = T^* - 2k^{*2} E^* \quad (8)$$

Where $T = T^* (\frac{\nu}{\eta})^3$, $E = E^* (\frac{\nu^2}{\eta})$ and $t = t^* (\frac{\eta^2}{\nu})$.

For the passive scalar the Batchelor scaling (indicated by $+$) introduces the length scale $\eta_B = \frac{\eta}{\sqrt{Sc}}$; the scaled spectrum and transfer are $E_\theta(k) = E_\theta^+(k^+) (\frac{\chi \eta^2 \eta_B}{\nu})$ and $T_\theta(k) = T_\theta^+(k^+) (\frac{\chi \eta^2}{\eta_B Sc})$ ($\chi = 2\nu_\theta \int k^2 E_\theta(k) dk$) giving the following dimensionless equation

$$\frac{\partial E_\theta^+}{\partial t^*} = T_\theta^+ - 2k^{*2} E_\theta^+ \quad (9)$$

Note that the Reynolds and Schmidt number dependencies do not appear explicitly in Eqs(8) and (9).

RESULTS

Here we focus on small to moderate Reynolds numbers. In the former case, R_λ is around 60, for which a well resolved pseudospectral simulation in a box of dimensions 2π and a 512^3 grid is available (Wray (1998)). Previous finite difference results with a 240^3 grid at R_λ approximately 46 were used in other papers to analyse the Sc dependence. Here, a new set of results with a 270^3 grid at a R_λ close to that

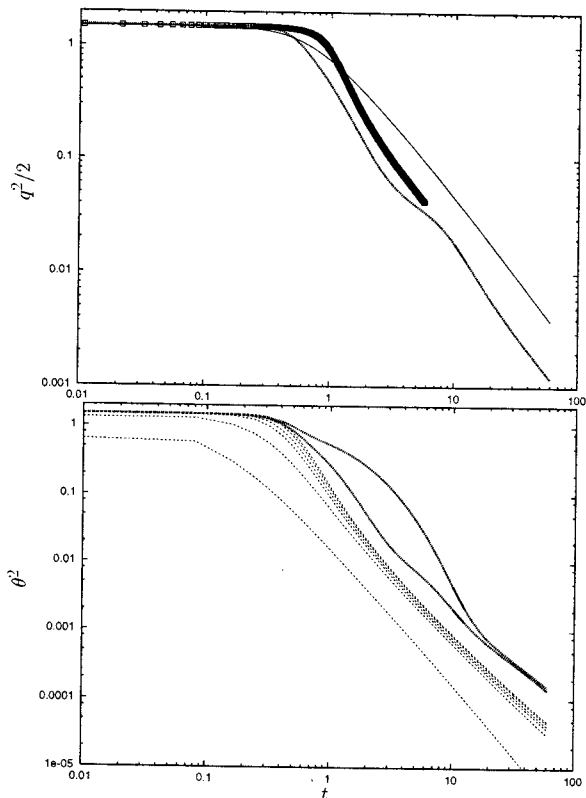


Figure 1: Time history of (a) Velocity rms and (b) scalar rms . Thin lines EDQNM, thick lines finite differences DNS, symbols pseudospectral DNS.

of Wray is used. The simulations include passive scalars for two values of Sc (1 and 3). Since the ability of second-order finite difference methods to yield accurate results has been under a cloud, we would like to show that this scepticism is not justified. In addition, we find that EDQNM yields, at the same R_λ as for the DNS, adequate results. The time evolution of $q^2/2$ depends on the numerical method used; for DNS, there is generation of very energetic nonphysical unresolved small scales that are dissipated differently. Following the initial transient period, all simulations reach a power-law decay behaviour, as shown in Fig.1a. Wray evolved the simulations for a relatively short time following the onset of the $q^2 \approx t^{-n}$ regime. The present finite difference simulation evolved up to $t = 60$ power-law region extending between $t=20$ and $t=60$ (i.e. the range is about a factor of 3 larger than that observed in Wray's database). In EDQNM, due to the increase in the highest value of k , the energy build-up does not occur and, consequently, the transient is more physical than in DNS. In addition, EDQNM can evolve for relatively long times before changes in the power-law decay are discernible. DNS and EDQNM show (Fig.1b) that, after the transient, and independently of Sc (except for $Sc \ll 1$), all distributions of θ^2 decay with values of m approximately equal to -1.4 for DNS and -1.6 for EDQNM.

Small Reynolds number ($R_\lambda \approx 60$)

Fig.2a shows that Kolmogorov-normalized energy spectra, obtained by the finite difference DNS and by EDQNM, compare well with those from pseudospectral simulations over a large range of wavenumbers. We have reported spectra at two instants; the pile-up in the pseudospectral simulations is due to the dealiasing procedure. The EDQNM generates spectra with a more rapid exponential decay than

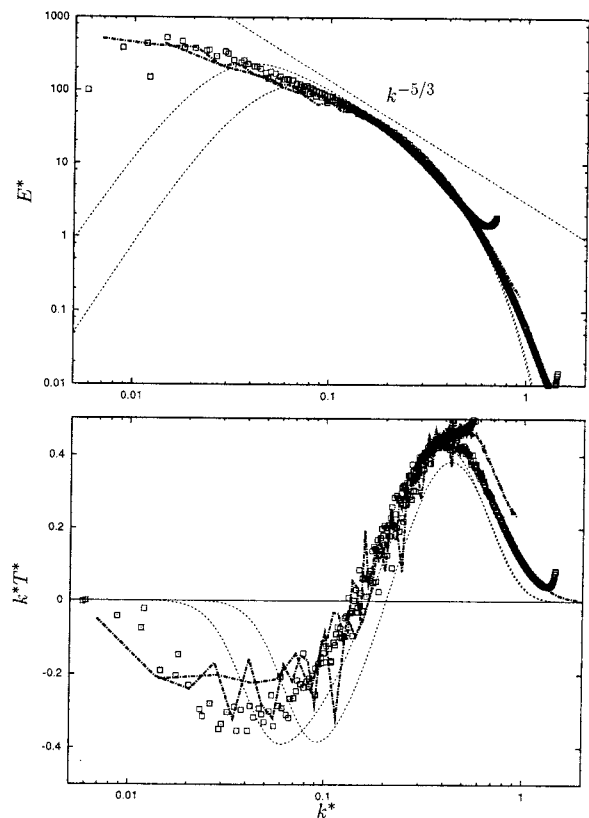


Figure 2: Profiles of (a) Spectra and (b) transfer at $R_\lambda \approx 60$. Thin dashed lines EDQNM, thick lines finite differences DNS, symbols pseudospectral DNS.

for DNS. This decay does not depend on the number of octaves and on the accuracy used for the triadic integral calculation. In addition, the best results are obtained with a local damping, as discussed previously. The exponential range in both EDQNM and DNS does not vary with time and does not change with ν .

Corresponding to the spectra in Fig.2a, Fig.2b shows that Kolomogorov-normalized distributions of $kT(k)$ agree with each other satisfactorily. In particular, EDQNM gives results in agreement with those from DNS, so there is hope that this theory can be used to study the behavior at large R_λ .

We are also interested in testing the Batchelor scaling for the scalar. The finite difference DNS at this small R_λ was performed for two values of Sc (1 and 3). Antonia & Orlandi (2003b) showed that at an even lower Re , the finite difference results agree with those from a pseudospectral method. The EDQNM was used to evolve six scalar fields, each with a different Sc (0.01, 0.1, 1, 3, 10, 20). Fig.3a shows that at the same t as in Fig.2, the collapse of the scalar spectra is rather good and the EDQNM results agree with those from DNS. EDQNM allows simulations at higher Sc with a significant k^{-1} range. The appearance of this region begins near $Sc = 1$ and continues to extend as Sc increases. For the scalar at various values of Sc , the spectra do not collapse perfectly in the exponential region; the collapse of the scalar transfer functions (Fig.3b) is worse. This can be explained by considering that k^+T^+ , around $k^+ = 1$, should balance $k^{3+}E^+$, and then, after multiplying by k^{3+} , the small differences for the scaled spectra in Fig.3a are enhanced.

However, Fig.3b shows satisfactory agreement between DNS and EDQNM scalar transfer functions; the positive and negative peaks do not vary appreciably with Sc ; further, all

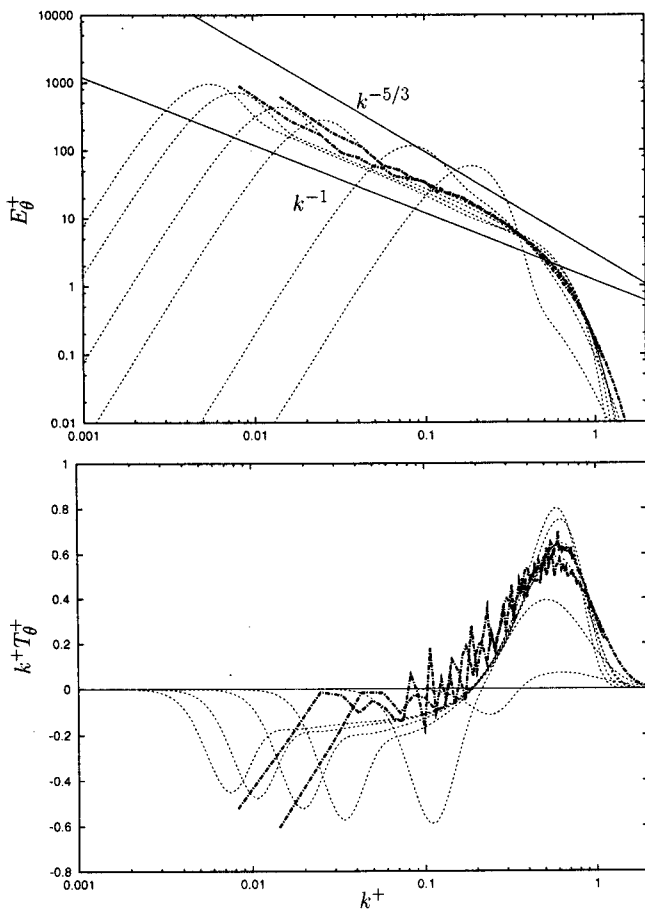


Figure 3: Profiles of (a) dimensionless scalar spectra and (b) scalar transfer at $R_\lambda \approx 60$; thin lines EDQNM at $Sc = 0.01, 0.1, 1, 3, 7, 20$; tick lines finite difference DNS at $Sc = 1, 3$

simulations show that the transfer is approximately constant across the k^{-1} range. Collapse of the transfer functions does not occur for $Sc \ll 1$ and it seems that for EDQNM, there is a weak increase of the maximum value with Sc . Despite these small discrepancies, we can state that the agreement is adequate. The formation of a substantial k^{-1} range in decaying turbulence has not been evident in DNS results, apparently because large values of Sc are not readily achievable with DNS. Lesieur *et al.* (1987), using EDQNM, observed this inertial diffusive range but in connection with an inertial range. They did not show spectra at low Reynolds numbers and different Sc nor was the presence of a k^{-1} range checked for a weak velocity field. We reiterate that Batchelor thought that a weak field is sufficient for generating the compressive strain rate that produces sharp scalar gradients at high Sc . We are nevertheless satisfied that EDQNM can reproduce part of the complex physics of interest to several applications where a passive scalar plays an important role. We have found that when $R_\lambda = 5$ and $Sc = 20$, there is no k^{-1} range. The latter only begins to form at $R_\lambda = 15$.

Moderate Reynolds number ($R_\lambda \approx 220$)

At present, only LES provides access to high Reynolds numbers, but it cannot be used to test different types of scaling due to the lack of a dissipation range. The only alternative is EDQNM. For example, by increasing ν by a factor of 20, R_λ is ≈ 220 at $t = 60$. The energy spectrum in Fig.4a shows a relatively long inertial range close to that

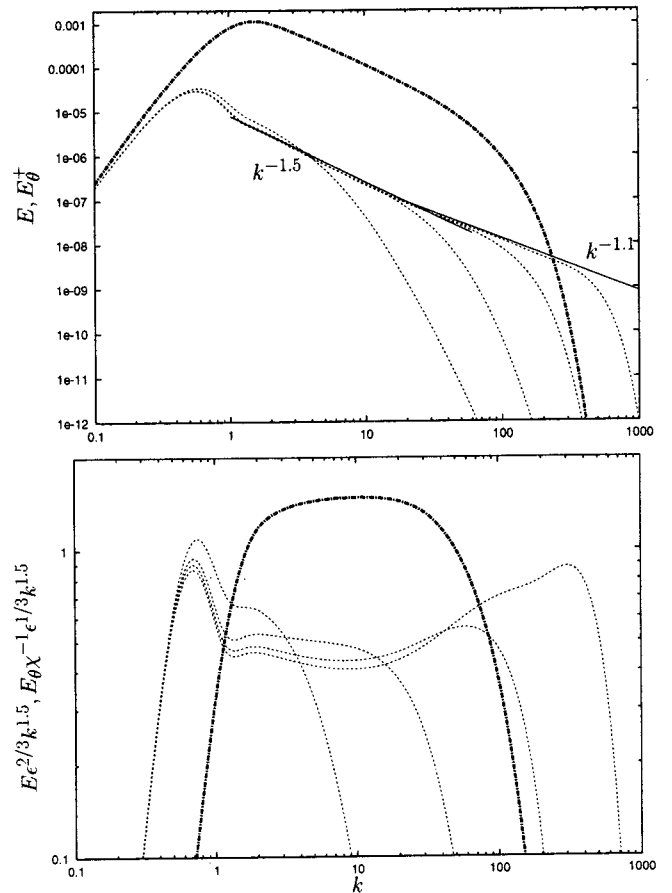


Figure 4: Profiles of (a) energy and scalar spectra and (b) compensated spectra at $R_\lambda \approx 220$; thin lines scalar at $Sc = 0.01, 0.1, 1, 10$; tick lines energy

displayed in several classical textbooks. For instance, Tennekes & Lumley (1972) described qualitatively the behavior of scalar spectra for $Sc \ll 1$ and $Sc \gg 1$. We have used four values of $Sc = 0.01, 0.1, 1, 10$, realising that the smallest and largest of these only poorly approximate the previous inequalities. Fig.5a shows that, because of our initial conditions, both the energy and scalar spectra grow quartically at low k . All scalars show a maximum at the same wavenumber (k_M) and their values do not depend on the Schmidt number. For $Sc \ll 1$, the dissipation range begins near k_M . For $Sc = 0.1$, a very short equilibrium range appears. At $Sc = 1$, it is of comparable extent to the energy inertial range. At $Sc = 1$, a very short viscous diffusive range forms, which expands for $Sc > 1$. At this point, we would like to point out that EDQNM gives inertial and inertial diffusive ranges with slopes (1.5 and 1.1) that differ from the theoretical predictions. This is not related to our time integration scheme or the accuracy of the triadic integral calculation but is related to the EDQNM closure. In the figures of Lesieur *et al.* (1987), differences in slope are also detectable, especially if compensated spectra are plotted, as in Herring (1990). Clearly, the results could depend on the value of the constant $C_\lambda (= 0.36)$, but it is interesting, if not surprising, that the EDQNM can predict the approach towards $k^{-5/3}$ as the Reynolds number is increased.

Fig.4b shows compensated spectra, evaluated by multiplying $E(k)$ and $E_\theta(k)$ by $k^{1.5}$. The resulting Kolmogorov constant is about 1.5 whereas the Obukhov-Corrsin constant is about 0.5. These values happen to be as reported by Tennekes & Lumley. Sreenivasan (1995,1996) reviewed

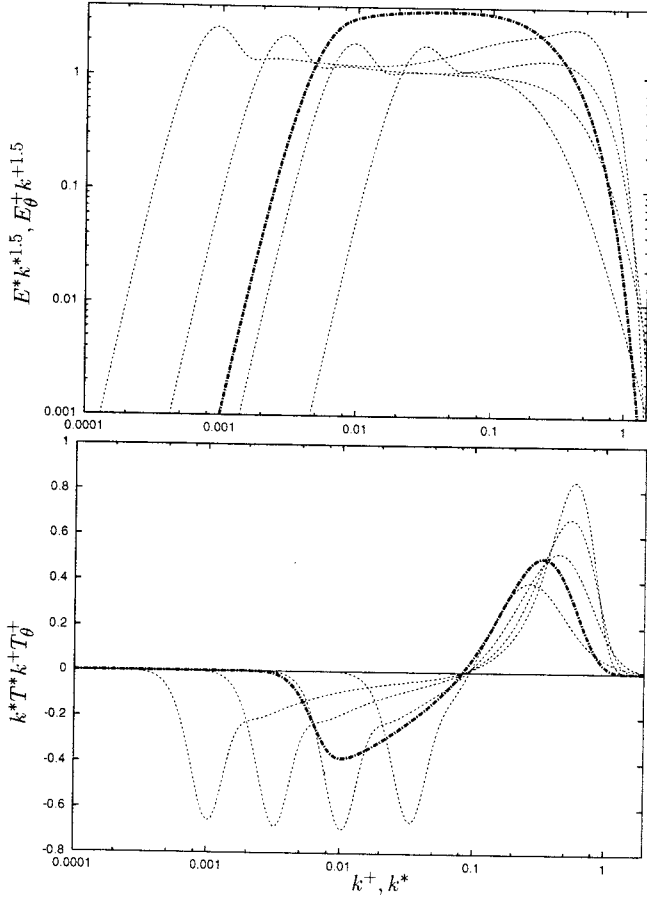


Figure 5: Profiles of dimensionless (a) energy and scalar spectra and (b) transfers at $R_\lambda \approx 220$; thin lines scalar at $Sc = 0.01, 0.1, 1, 10$; tick lines energy

a large number of experimental results for these constants, as inferred mainly from one-dimensional spectra. The corresponding values for the constants associated with three-dimensional spectra are essentially as found here. In the theoretical case, when the inertial range of the energy and of the scalar spectra decay as $k^{-5/3}$, the dimensional arguments show that the constants inferred from $E^*(k^*)$ and $E_\theta^+(k^+)Sc^{1/3}$ are identical to those estimated from $E(k)$ and $E_\theta(k)$. In our case, EDQNM yields a $k^{-1.5}$ region and the constants are different. Figs.4b and 5a exhibit this difference but, at the same time, Fig.5a shows a rather satisfactory scaling of the compensated spectra at different Sc as well as the variation of slope of the inertial-diffusive range.

The inertial ranges can be theoretically evaluated, following the arguments in Tennekes & Lumley (1972), by assuming that the transfer functions are constant. At the present moderate Reynolds number, the transfer functions, $T(k)$ and $T_\theta(k)$, even if appropriately scaled, indicate large negative values at small k . It is more useful to plot $k^+T^+k^+$ and k^*T^+ , as in Fig.5b. The positive and negative contributions are similar. At low k , EDQNM indicates that the large scales are almost independent of the diffusivity, in accord with the time history of θ^2 in fig.1a; the imperfect collapse of the maximum and its weak dependence on Sc is related to the small influence of Sc on the decay of the exponential range.

We can conclude that for a moderately large Re , EDQNM allows to qualitatively describe the evolution of the flow and to predict the different slopes in the inertial and in the inertial-diffusive ranges.

SCALAR STRUCTURES

An interesting analysis of the structure of the passive scalar at different Sc was given by Brethouwer *et al.* (2002) when a mean scalar gradient is present. Even in this case, when an anisotropy is imposed by the external field, the compressive strain produces sharp gradients of the scalar thus causing the scalar field to be more intermittent than the velocity field. Here, we are interested in identifying the regions of the scalar structures which contribute to the scalar transfer by analyzing the individual contribution of each term in the transport equation for θ^2 , viz.

$$\frac{\partial \theta^2 / 2}{\partial t} = -\theta \frac{\partial \theta u_j}{\partial x_j} - \nu_\theta \left(\frac{\partial \theta}{\partial x_j} \right)^2 + \nu_\theta \nabla^2 \theta^2 / 2. \quad (10)$$

The term which corresponds to T_θ in physical space is the third-order structure function $D_{L\theta\theta}(r)$. This latter term was analyzed in some detail by Orlandi & Antonia (2002). Here, our objective is to investigate how the structures associated with θ^2 affect the first term on the RHS ($T_a = -\theta(\partial \theta u_j / \partial x_j)$ of Eq(10)). The second term, always negative, is the scalar dissipation rate whilst the last term ($T_r = \nu_\theta \nabla^2 \theta^2 / 2$) is related to the curvature of the scalar gradient regions. The first and third terms can be positive and negative so that their total contribution to the evolution of θ^2 is negligible. Fig.6a shows the pdfs of $\sigma_a = T_a / \langle T_a^2 \rangle^{1/2}$ and of $\sigma_r = T_r / \langle T_r^2 \rangle^{1/2}$. We note that these terms are very intermittent, confirming the EDQNM results of Crocco & Orlandi, 1985, i.e. non-local triadic interactions are highly localized and intense. Fig.6a shows that, for a large number of points in the field, T_a is small and there is a very small probability that it can reach twice its rms value. The trend of the curvature-related term implies that, over a large part of the field, high concentrations of the scalar reside in elongated, thin structures. These are locations where high scalar gradients occur as a result of the compressive strain rate. Regions with very high positive and negative curvature, driven by localized and intense vorticity, are very rare.

The joint probability density function between σ_r and σ_a in Fig.6b allows the focus to be on regions of the scalar which contribute significantly to the scalar transfer. We see that structures with negative curvature contribute more positively; in these regions, the decrease in θ^2 is smaller than expected from the local scalar dissipation rate. This scenario is inverted when the curvature is of opposite sign. The structures with positive curvature contribute positively to the transfer and Fig.6b indeed shows that the contribution from terms of the same sign is smaller than that when they have opposite signs.

Although the figures shown here are for $Sc = 0.7$, the results do not change significantly with Sc (since each term was normalized by its rms value).

CONCLUSION

The influence of the Schmidt number on the decay of a passive scalar is of interest in practical applications and in theoretical considerations. It is however impossible to understand the underlying complex physics by using only one approach. In this paper, the focus has been entirely on numerical experiments and simulations which use closures. Some of the theoretical considerations about scaling and the cascading of energy and the scalar variance from large to small scales cannot be studied with DNS when the Reynolds number is large. We have therefore used the EDQNM spectral closure. Both techniques indicated that Kolmogorov and

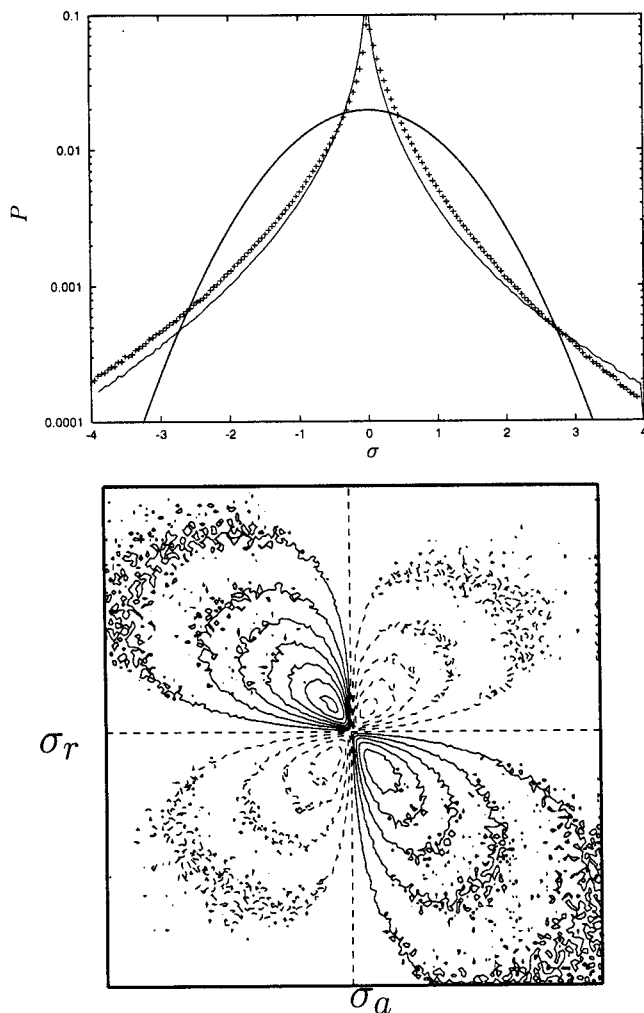


Figure 6: Pdf of $\times \sigma_r$ — σ_a (a) and Joint pdf of σ_r and σ_a (b) at $Sc = 0.7$.

Batchelor variables provide an effective collapse of the high wavenumber range of the energy and scalar spectra. In addition, the numerical techniques have shown very clearly the different ranges that exist in the spectra and how they are related to the transfers from large to small scales. These two aspects can contribute to improving the modeling of small scales in LES for combustion related applications. Clearly, inadequacies relating to the spectral closure remain; hopefully, they should motivate future attempts at reproducing the theoretical predictions at very high Reynolds numbers.

The transfer of a scalar in wavenumber space has been related to the corresponding terms in physical space, leading to the conclusion that most of the scalar structures are elongated but that high curvature regions are rare. Nonetheless, the latter may be important since, in combustion, they are usually associated with flame extinction.

ACKNOWLEDGMENTS

RAA acknowledges the support of the Australian Research Council, P.O. the support of MURST 60%. We are very grateful to Alan Wray for providing us with his pseudospectral code.

REFERENCES

Antonia R.A. & Orlandi, P. 2003a. "On the Batchelor

Constant in Decaying Isotropic Turbulence", submitted to *Phys. Fluids*.

Antonia R.A. & Orlandi, P. 2003b. "Effect of Schmidt number on small-scale passive scalar turbulence", to appear in *Applied Mechanics Reviews*.

Brethouwer, G. Hunt, J.C.R. & Nieuwstadt, F. T. M. 2002, "Micro-structure and Lagrangian statistics of the scalar field with a mean gradient in isotropic turbulence", *J. Fluid Mech.* Vol. 474, pp.193 - 225 .

Crocco, L. & Orlandi, P. 1985. "A transformation for the energy-transfer term in isotropic turbulence", *J. Fluid Mech.* Vol. 161, pp.405-424.

George, W.K. 1992a "The decay of homogeneous isotropic turbulence", *Phys. Fluids A*, Vol 4 (7), pp1492-1509

George, W.K. 1992b "Self-preservation of temperature fluctuations in isotropic turbulence", in *Studies of turbulence* (eds T B Gatsky, S Sarkar & G Speziale) Springer Verlag pp.514-528.

Herr, S., Wang, L.P. & Collins, L.R., 1996, "EDQNM model of a passive scalar with a uniform mean gradient" *Phys. Fluids* , Vol. 8 (6), pp.1588-1607.

Herring, J.R. 1990. "Comparison of closure to spectral-based large eddy simulations", *Phys. Fluids A*, Vol. 2 (6), pp.979-983.

Herring, J.R. & Kraichnan, R. H. 1972. "Comparison of some approximations for isotropic turbulence", in *Statistical models and turbulence* (ed. M. Rosenblatt & C. Van Atta) Lecture Notes in Physics Springer Verlag, Vol. 12, pp.146-194.

von Karman, T. & Howarth, L., 1938, "On the statistical theory of isotropic turbulence" *Proc. R.Soc. London Ser. A* 164, Vol.917, pp.192-215.

Lesieur, M. (1997) *Turbulence in fluids* 3rd rev. and enlarged ed. Dordrecht, Kluwer.

Lesieur, M., Montmory, C. & Chollet, J.P. 1987. "The decay of kinetic energy and temperature variance in three-dimensional isotropic turbulence", *Phys. Fluids*, Vol. 30 (5), pp. 1278-1286.

Mydlarski L. and Warhaft Z. (1996) "On the onset of high-Reynolds-number grid-generated wind tunnel turbulence" *J. Fluid Mech.*, Vol 320, pp 331-368.

Orlandi, P. 2000. *Fluid Flow Phenomena : A Numerical Toolkit*, Dordrecht, Kluwer.

Orlandi, P. Antonia R.A. 2002. "Dependence of the non-stationary form of Yaglom's equation on the Schmidt number", *J. Fluid Mech.* Vol. 451, pp.99-108.

Orszag, S.A., 1970, "Analytical theories of turbulence", *J. Fluid Mech.* Vol. 41, pp.363-386.

Sreenivasan, K. R. 1995 "On the universality of the Kolmogorov constant" *Phys. Fluids* Vol.7(11), pp.2778-2784.

Sreenivasan, K.R. 1996 "The passive scalar spectrum and the Obukhov-Corrsin constant" *Phys. Fluids* Vol.8(1) pp.189-196.

Tennekes, H. and Lumley, J.L. 1972, *A first course in Turbulence*, M.I.T., Cambridge.

Wray, A. 1998 "Decaying isotropic turbulence", in *AGARD Advisory Report* Vol. 345, pp.63-64.